Reimagine BiSeNet for Real-Time Domain Adaptation in Semantic Segmentation

This is the author's version of the article that has been presented at IEEE ISCAS2019
The editorial version of the paper is available at http://dx.doi.org/10.1109/ISCAS.2019.8702181

Tuning a Resonant dc/dc Converter on the Second Harmonic for Improving Performance: a Case Study

Fabio Pareschi*,§, Raul Blecic†, Mauro Mangia§ Adrijan Baric†, Riccardo Rovatti‡,§, and Gianluca Setti*,§
* DET – Politecnico of Torino, corso Duca degli Abruzzi 24, 10129 Torino, Italy.
email:{fabio.pareschi, gianluca.setti}@polito.it
† Faculty of Electrical Engineering and Computing – University of Zagreb, Unska 3, 10000 Zagreb, Croatia.
email:{raul.blecic, adrijan.baric}@fer.hr
‡ DEI – University of Bologna, viale Risorgimento 2, 40136 Bologna, Italy. email: riccardo.rovatti@unibo.it
§ ARCES – University of Bologna, via Toffano 2/2, 40125 Bologna, Italy. mauro.mangia@unibo.it

***Abstract*—A recent paper improved the state of the art for resonant class-E dc/dc converters by relaying their design on the solution of an associated non-linear dimensionless mathematical system. We show in this paper that when the associated non-linear system can be solved, the solution is not always unique. By considering a simple case study we are able to compute two different solutions leading to two different designs. In the first one the main spectral component of voltage and current waveforms is located around the first clock harmonic, and around the second harmonic in the other solution. Interestingly, the latter design leads to a reduction either in the size of inductors/transformers or in the oscillation frequency (a 2.46x factor), and also a non-negligible improvement in the converter efficiency (from 74.1% to 75.8%).**

I. Introduction

Resonant switching dc/dc converters have been introduced with the aim of increasing the system power density [1] by reducing passive element size, in particular the magnetic ones (inductors and transformers). To reach this goal, converters are designed to operate in the VHF range $30-300$ MHz [2], [3] by exploiting radio frequency (RF) amplifier design techniques [1], [4] .

The key point is the so called *soft switching* approach: reactive elements are designed to properly shape the voltage and current waveforms and so reduce the voltage-current product on switching devices (either controlled or not) at the switching instants [5], [6], [7]. In this way it is possible to reduce thermal stress and the switching loss impact that are present in conventional class-D topologies (the *hard-switching* approach) when operating at high frequencies.

In this paper we focus on the class-E dc-dc converter analyzed in [8] and depicted in Fig. 1. The converter can be divided into an inverter section (the part of the circuit including the MOS as controlled switch) and a rectifier one (the part including the diode as uncontrolled switch), connected by means of an isolation transformer. To fulfill the optimal class-E condition requirements, the voltage $V_{C_{\rm inv}}(t)$ across the MOS switch should go to zero with zero-time-derivative immediately before the MOS turn-ON instant thus lowering (ideally, down to zero) the switching loss with beneficial effects also in terms of EMI emission [9], making it, from this point of view, a valid alternative with respect to spread-spectrum clocking techniques [10][11]. These soft-switching techniques are known as *Zero-Voltage Switching (ZVS)* and *Zero-Voltage-Derivative Switching (ZVDS)* respectively.

In [8] an innovative and exact design procedure for the converter of Fig. 1 has been proposed, improving the state of the art in class-E resonant converter design based on strong simplifying assumptions [3], [12]. In more detail, the design of the converter is achieved as the de-normalization of the solution of a dimensionless non-linear associated system. Even if the authors of [8] were able to prove the existence of a solution for a wide range of parameters, the problem of the uniqueness of the solution has not been considered.

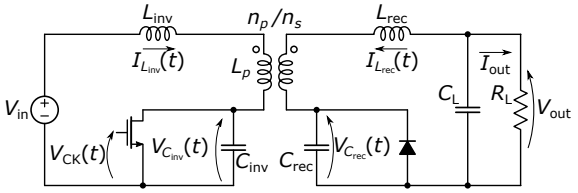

Fig. 1. Schematic of the class-E converter analyzed in [8] and considered in this paper.

We show here that this system may actually present more than one solution. We will detail a case study where we are able to find two solutions. The first one is related to the standard behavior, where all voltage and current waveforms oscillate at the same frequency f_s as the main clock $V_{\rm CK}(t)$. This is the common assumption adopted by the entire literature on resonant converters. Conversely, designing the converter according to the second solution leads to a circuit where voltage and current waveforms feature two oscillations during one clock period. We refer to this solution as the second harmonic solution.

Tuning an RF amplifier on the second (or higher) harmonic is a topic that has been sometimes considered in the literature [13]. However, to the best of our knowledge, it is an undiscovered topic in resonant dc/dc converters. The only approach that may be considered similar is the design of the Φ_2 converter [14], where additional reactive elements are used to give a double-oscillation shape to $V_{C_{\rm inv}}(t)$ and reduce its peak value, thus reducing the voltage stress on the MOS switch. However, all other waveforms feature a single oscillation per clock period.

In the proposed case study, the design based on the second harmonic solution leads to two advantages. The first one is the possibility to reduce either the size of the magnetic elements, or the oscillation frequency. The second advantage is a non-negligible increase in the converter efficiency. This reveals that the second harmonic solution in resonant converters is a topic that is worth further investigation.

The paper is organized as follows. In Section II we recall the normalized non-linear mathematical model proposed in [8].

This is the author's version of the article that has been presented at IEEE ISCAS2019
The editorial version of the paper is available at http://dx.doi.org/10.1109/ISCAS.2019.8702181

In Section III we compare the first and the second harmonic solution from a theoretical point of view, while in Section IV we propose SPICE simulation results on a case study of the same converter designed according to the two solutions. Finally, we draw the conclusion.

II. The normalized mathematical model

We propose in this section a summary on the steps necessary to derive the non-linear system associated to the converter of Fig. 1. Since our aim is to deal with the schematic of Fig. 1 only, we slightly reduce the complexity of the notation with respect to the original and more general approach in [8].

1. The capacitance $C_{\rm L}$ is assumed large enough to consider $V_{\rm out}$ constant, with $V_{\rm out} = R_{\rm L} I_{\rm out}$.

2. All elements in Fig. 1 are considered *lossy*. Inductors $L_{\rm inv}$ and $L_{\rm rec}$, and capacitors $C_{\rm inv}$ and $C_{\rm rec}$ are modeled by the standard series-resistance equivalent circuit for lossy reactive elements operating at angular frequency $\omega_s = 2\pi f_s$, where the series-resistance is expressed by means of the quality factor, respectively

$$Q_{L_{\rm inv,rec}} = \frac{\omega_s L_{\rm inv,rec}}{R_{L_{\rm inv,rec}}},\ Q_{C_{\rm inv,rec}} = \frac{1}{\omega_s C_{\rm inv,rec} R_{C_{\rm inv,rec}}}.$$

The transformer is described by means of the coupling factor k and the turns ratio n_s/n_p: indicating with L_p the inductance seen at the primary side (with $L_s = L_p(n_s/n_p)^2$ the inductance at the secondary side), the transformer is modeled by a core inductor kL_p (or kL_s at the secondary side) and two leakage inductors $(1-k)L_p$ (or $(1-k)L_s$ at the secondary side). These three inductors are considered with a quality factor Q_{L_x}. The MOS switch is considered an ideal open circuit when off, and a resistance $R_{DS}^{\rm ON}$ when on. The rectifying diode is considered an ideal open circuit when off, and the series of a voltage source $V_D^{\rm ON}$ and a resistance $R_D^{\rm ON}$ when on. Finally, two additional resistances $R_{\rm in}$ and $R_{\rm out}$ are considered to take into account any other possible loss in the inverter and the rectifier loop, respectively.

3. The transformer is removed by considering the equivalent circuit at the primary side depicted in Fig. 2.

4. The evolution of the circuit of Fig. 2 is regulated by the four state variables $I_{L_{\rm inv}}(t)$, $I_{L_{\rm rec}}(t)$, $V_{C_{\rm inv}}(t)$ and $V_{C_{\rm rec}}(t)$. Indeed, it is convenient to consider their normalized counterparts (both in time and amplitude)

$$\begin{aligned} i_{L_{\rm inv}}(\theta) &= \frac{n_p}{n_s}\frac{I_{L_{\rm inv}}(\theta/\omega_s)}{I_{\rm out}}, \quad i_{L_{\rm rec}}(\theta) = \frac{I_{L_{\rm rec}}(\theta/\omega_s)}{I_{\rm out}}, \\ v_{C_{\rm inv}}(\theta) &= \frac{n_s}{n_p}\frac{V_{C_{\rm inv}}(\theta/\omega_s)}{V_{\rm out}}, \quad v_{C_{\rm rec}}(\theta) = \frac{V_{C_{\rm rec}}(\theta/\omega_s)}{V_{\rm out}}. \end{aligned} \tag{1}$$

With these, and with some minor simplifying assumptions (such as that the $C_{\rm inv}$ and $C_{\rm rec}$ do not affect the circuit behavior when the MOS and the rectifying diode are on, respectively), the Kirchhoff equations of the circuit can be written as in (2). The binary variables $m^{\rm ON}$ and $d^{\rm ON}$ account for the MOS and the rectifying diode to be in the on or off state, respectively. The system is based on the dimensionless quantities

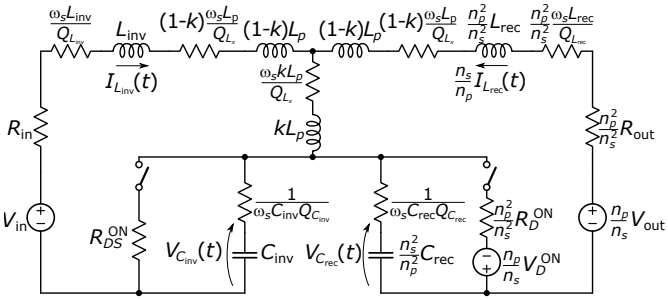

Fig. 2. Equivalent circuit at the primary side of considered class-E converter including all lossy elements.

$$\begin{aligned} q_i &= \frac{n_s^2}{n_p^2}\frac{1}{\omega_s C_{\rm inv} R_{\rm L}},\ q_r = \frac{1}{\omega_s C_{\rm rec} R_{\rm L}} \\ q_x &= k\frac{n_s^2}{n_p^2}\frac{\omega_s L_p}{R_{\rm L}} = k\frac{\omega_s L_s}{R_{\rm L}}, \\ k_i &= \frac{kL_p}{L_{\rm inv}+L_p},\ k_r = \frac{kL_s}{L_{\rm rec}+L_s}, \end{aligned} \tag{3}$$

on $Q_{C_{\rm inv}}$, $Q_{C_{\rm rec}}$, Q_{L_x}, and the generalized quality factors

$$g_{DS}^{\rm ON} = \frac{n_p^2}{n_s^2}\frac{R_{\rm L}}{R_{DS}^{\rm ON}},\ g_D^{\rm ON} = \frac{R_{\rm L}}{R_D^{\rm ON}},\ g_{\rm in} = \frac{n_p^2}{n_s^2}\frac{R_{\rm L}}{R_{\rm in}},\ g_{\rm out} = \frac{R_{\rm L}}{R_{\rm out}},$$

$$\frac{1}{Q_{L_{\rm i}}} = \frac{1}{Q_{L_{\rm inv}}}\frac{L_{\rm inv}}{L_{\rm inv}+(1-k)L_p} + \frac{1}{Q_{L_x}}\frac{kL_p}{L_{\rm inv}+(1-k)L_p},$$

$$\frac{1}{Q_{L_{\rm r}}} = \frac{1}{Q_{L_{\rm rec}}}\frac{L_{\rm rec}}{L_{\rm rec}+(1-k)L_s} + \frac{1}{Q_{L_x}}\frac{kL_s}{L_{\rm rec}+(1-k)L_s},$$

and on

$$\mu = \frac{n_s}{n_p}\frac{V_{\rm in}}{V_{\rm out}},\ v_D^{\rm ON} = \frac{V_D^{\rm ON}}{V_{\rm out}}.$$

5. System (2) is turned into four different non-linear systems, whose order ranges from 2 to 4 according to $m^{\rm ON}$ and $d^{\rm ON}$. The analytic solutions for all different systems can be computed. With these, by the knowledge of the MOS turn on and off instants and of the initial conditions $i_{L_{\rm inv}}^0$ and $i_{L_{\rm rec}}^0$, by computing the rectifying diode turn on and off instants, and by ensuring continuity of the main variables whenever a change in $m^{\rm ON}$ and $d^{\rm ON}$ is observed, it is possible to get an exact mathematical expression for $i_{L_{\rm inv}}(\theta)$, $i_{L_{\rm rec}}(\theta)$, $v_{C_{\rm inv}}(\theta)$ and $v_{C_{\rm rec}}(\theta)$ as the piece-wise combination of the solutions of (2) with the correct values of $m^{\rm ON}$ and $d^{\rm ON}$.

$$\begin{aligned} &\left(1-m^{\rm ON}\right)v_{C_{\rm inv}}(\theta) + \left(\frac{1}{g_{\rm in}} + \frac{1-k_i}{k_i}\frac{q_x}{Q_{L_{\rm i}}} + \frac{q_x}{Q_{L_x}} + \left(1-m^{\rm ON}\right)\frac{q_i}{Q_{C_{\rm inv}}} + \frac{m^{\rm ON}}{g_{DS}^{\rm ON}}\right) i_{L_{\rm inv}}(\theta) + \frac{q_x}{Q_{L_x}} i_{L_{\rm rec}}(\theta) + \frac{q_x}{k_i}\frac{{\rm d}i_{L_{\rm inv}}(\theta)}{{\rm d}\theta} + q_x\frac{{\rm d}i_{L_{\rm rec}}(\theta)}{{\rm d}\theta} = \mu \\ &\left(1-d^{\rm ON}\right)v_{C_{\rm rec}}(\theta) - d^{\rm ON}v_D^{\rm ON} + \frac{q_x}{Q_{L_x}} i_{L_{\rm inv}}(\theta) + \left(\frac{1}{g_{\rm out}} + \frac{1-k_r}{k_r}\frac{q_x}{Q_{L_{\rm r}}} + \frac{q_x}{Q_{L_x}} + \left(1-d^{\rm ON}\right)\frac{q_r}{Q_{C_{\rm rec}}} + \frac{d^{\rm ON}}{g_D^{\rm ON}}\right) i_{L_{\rm rec}}(\theta) + q_x\frac{{\rm d}i_{L_{\rm inv}}(\theta)}{{\rm d}\theta} + \frac{q_x}{k_r}\frac{{\rm d}i_{L_{\rm rec}}(\theta)}{{\rm d}\theta} = 1 \end{aligned} \tag{2}$$

$$i_{L_{\rm inv}}(\theta) = \frac{1}{q_i}\frac{{\rm d}v_{C_{inv}}(\theta)}{{\rm d}\theta} \quad (m^{\rm ON}=0 \text{ only}), \qquad i_{L_{\rm rec}}(\theta) = \frac{1}{q_r}\frac{{\rm d}v_{C_{rec}}(\theta)}{{\rm d}\theta} \quad (d^{\rm ON}=0 \text{ only})$$

This is the author's version of the article that has been presented at IEEE ISCAS2019
The editorial version of the paper is available at http://dx.doi.org/10.1109/ISCAS.2019.8702181

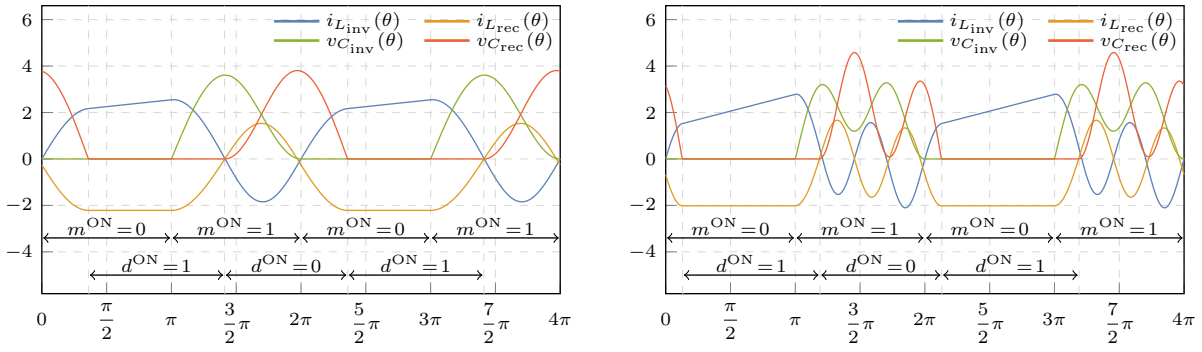

(a) (b)

Fig. 3. Normalized evolution of the lossless class-E converter with $k_i = 1$, $k_r = 0.8$, $\mu = 1$ according to the theoretical model ($i_{L_{\rm inv}}(\theta)$, $i_{L_{\rm rec}}(\theta)$, $v_{C_{\rm inv}}(\theta)$ and $v_{C_{\rm rec}}(\theta)$ are shown) for: (a) the first harmonic solution; (b) the second harmonic solution.

6. The design of the class-E converter is then tuned into a mathematical problem by asking that the converter, once stationary conditions are reached, operates with optimal class-E condition (ZVS and ZVDS)

$$\begin{cases} i_{L_{\rm inv}}(2\pi) = i^0_{L_{\rm inv}} \\ i_{L_{\rm rec}}(2\pi) = i^0_{L_{\rm rec}} \\ \dfrac{1}{2\pi}\displaystyle\int_0^{2\pi} i_{L_{\rm rec}}(\theta)\,{\rm d}\theta + 1 = 0 \\ v_{C_{\rm inv}}(\theta_{\rm SW}) = 0 \\ i_{L_{\rm inv}}(\theta_{\rm SW}) = 0 \end{cases} \tag{4}$$

where $\theta_{\rm SW}$ is the normalized time instant when the MOS is turned ON.

III. Solutions of the Mathematical Model

From a circuit point of view, the aim of the system (4) is clear. The first two equations set the continuity of the two current variables (with a proper choice of the time origin, it is not necessary to set continuity of the two voltage variables). The third one is necessary to deal with the assumption that $V_{\rm out}$ is constant. Recalling that, when $m^{\rm ON} = 0$, the $i_{L_{\rm inv}}(\theta)$ is given by the derivative of the $v_{C_{\rm inv}}(\theta)$, the last two equalities set ZVS and ZVDS, respectively.

It is interesting to consider (4) from a pure mathematical point of view. It is a system of 5 *non-linear* equations: in fact, despite the system (2) being linear, to properly combine the different solutions according to $m^{\rm ON}$ and $d^{\rm ON}$ it is required to compute the rectifying diode turn on and off instants. This makes the functions $i_{L_{\rm inv}}(\theta)$, $i_{L_{\rm rec}}(\theta)$ and $v_{C_{\rm inv}}(\theta)$ used in (4) non-linear.

By considering, as suggested in [8], the quantities q_i, q_r, q_x, $i^0_{L_{\rm inv}}$ and $i^0_{L_{\rm rec}}$ as design variables, and all other quantities as known parameters, (4) is a non-linear system of 5 equations in 5 variables. However, due to the non-linearity, proving either the existence and the uniqueness of a solution is a hard task that has not been investigated in [8].

Let us consider a dimensionless lossless system where $k = 1$, $v_D^{\rm ON} = 0$ and all quality factors are infinite. Let as also assume that $k_i = 1$, $k_r = 0.8$ and $\mu = 1$. Note that $k_i = k$ is an interesting choice, since it allows $L_{\rm inv} = 0\,{\rm H}$. Let us also assume $\theta_{\rm SW} = \pi$, i.e., a 50% duty cycle clock. Using these parameters, a solution of (4) is

$$q_i = 1.67,\ q_r = 2.22,\ q_x = 5.34,\ i^0_{L_{\rm inv}} = 2.55,\ i^0_{L_{\rm rec}} = -2.21 \tag{5}$$

The normalized waveforms obtained using this solution are depicted in Fig. 3-(a) along with the values of $m^{\rm ON}$ and $d_{\rm ON}$. The shape of these waveforms is commonly observed in resonant converters.

Indeed, an additional solution can be found as

$$q_i = 2.67,\ q_r = 5.09,\ q_x = 2.17,\ i^0_{L_{\rm inv}} = 2.78,\ i^0_{L_{\rm rec}} = -2.02 \tag{6}$$

that gives rise to the normalized waveforms in Fig. 3-(b).

From a visual point of view, there is a clear difference. Waveforms in (5) feature a single oscillation in one clock period. We refer to this as the first harmonic solution. Conversely, waveforms from (6) feature two oscillations during one clock period. We refer to this as the second harmonic solution. Even if we were not able to identify them, we cannot exclude the possibility that higher order solutions exist.

Apart from the visual difference, it is interesting to evaluate possible advantages of the first and of the second solution. The second harmonic solution is obtained with a q_x that is about $2.5\times$ smaller with respect to the first harmonic solution. According to (3), at a given load capability (i.e., assuming a constant $R_{\rm L}$), a smaller q_x is reflected in:

- a smaller L_p and L_s (and consequently smaller $L_{\rm inv}$ and $L_{\rm rec}$ assuming fixed k_i and k_r) at a given ω_s;
- a smaller ω_s at a given L_p, L_s.

In other words, the second harmonic solution allows either a minimization of the inductors size or a lower working frequency. This is clearly beneficial: we recall that the main reason why resonant converters have been introduced is to allow a reduction in the magnetic elements size for miniaturization purposes [5].

Another positive aspect of the second harmonic solution is the lower RMS value of the two currents. For the first harmonic solution we have

$$\left(i^{\rm RMS}_{L_{\rm inv}}\right)^2 = 3.39,\ \left(i^{\rm RMS}_{L_{\rm rec}}\right)^2 = 2.88$$

and for the second harmonic

$$\left(i^{\rm RMS}_{L_{\rm inv}}\right)^2 = 3.19,\ \left(i^{\rm RMS}_{L_{\rm rec}}\right)^2 = 2.61.$$

According to the modeling of Fig. 2, two types of power losses can be found. The first is on the diode, and using (1) can be expressed as

$$P_D \approx V_D^{\rm ON} I_{\rm OUT} = v_D^{\rm ON} P_{\rm out}$$

This is the author's version of the article that has been presented at IEEE ISCAS2019
The editorial version of the paper is available at http://dx.doi.org/10.1109/ISCAS.2019.8702181

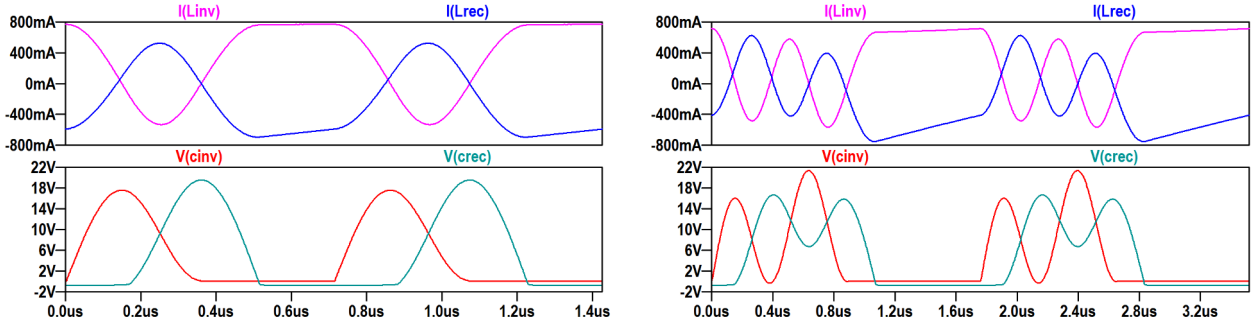

Fig. 4. SPICE simulation of the case-study class-E converter: (a) first harmonic solution; (b) second harmonic solution.

while the loss on the parasitic resistance depends on the loss resistance $R_{\rm loss}$ and the current flowing in it, and come in one of the two forms

$$P_R \approx R_{\rm loss}\left(I^{\rm RMS}\right)^2 = \begin{cases} \dfrac{n_s^2}{n_p^2}\dfrac{R_{\rm loss}}{R_{\rm L}}\left(i_{L_{\rm inv}}^{\rm RMS}\right)^2 P_{\rm out} \\ \dfrac{R_{\rm loss}}{R_{\rm L}}\left(i_{L_{\rm rec}}^{\rm RMS}\right)^2 P_{\rm out} \end{cases}$$

depending if we are considering a loss in the inverter or rectifier loop.

While the first kind of loss is constant, the second one is smaller for the second harmonic solution due to the lower RMS value of the current signals. The beneficial effect is a reduced energy power loss, especially in the magnetic elements, that could also result in an improved converter efficiency assuming that the diode losses are not dominant with respect to resistive losses.

IV. Simulation Results

We provide in this section SPICE simulation results for a 5 V-to-5 V converter with $I_{\rm out} = 240\,{\rm mA}$ design both according to the first and the second harmonic solutions. For a fair comparison we use the same elements for all converters.

In detail, we use a *WE-FLEX* transformer by Würth Elektronik in $n_s/n_p = 1$ configuration. This transformer has $L_p = 8.7\,\mu{\rm H}$, a coupling coefficient $k \approx 0.98$ and, according to [8], a quality factor $Q_{L_x} \approx 45$ at $f_s = 1\,{\rm MHz}$. We also force $L_{\rm inv} = 0\,{\rm H}$, while $L_{\rm rec} = 2.2\,\mu{\rm H}$ is a wire-wound chip inductor whose quality factor is around $Q_{L_{\rm rec}} \approx 50$ for $f_s = 1\,{\rm MHz}$. We also assume to work far from the inductor self-resonant frequency, so that Q_{L_x} and $Q_{L_{\rm rec}}$ are increasing with the frequency [2], [15]. We assume ideal capacitors, as ceramic capacitors with C0G dielectric ensure extremely high performance (quality factor > 1000). Furthermore, we use a IRLML0030TR N-MOS transistor by International Rectifier as the MOS switch and a ES1B by Vishay as the rectifying diode. According to SPICE results, for the given working point we propose to model them with $R_{DS}^{\rm ON} \approx 0.03\,\Omega$, $V_D^{\rm ON} \approx 0.7\,{\rm V}$ and $R_D^{\rm ON} \approx 0.2\,\Omega$. For all devices, except capacitors and $L_{\rm rec}$, we use SPICE models provided by the manufacturer. We also take into account additional losses such as circuit trace losses, contact losses, or input voltage source internal resistance by means of $R_{\rm in} = 0.1\,\Omega$ and $R_{\rm out} = 0.1\,\Omega$.

With these elements, we have

$$k_i = 0.98,\ k_r = 0.78,\ \mu = 1,\ Q_{L_{\rm i}} = Q_{L_x},\ Q_{L_{\rm r}} \approx Q_{L_{\rm rec}},$$
$$v_D^{ON} \approx 0.14,\ g_{DS}^{\rm ON} \approx 690,\ g_D^{\rm ON} \approx 140,\ g_{\rm in} = g_{\rm out} \approx 210.$$

These values are similar to that considered in the previous section, and give rise to two solutions. The first harmonic one is

$$q_i = 1.38,\ q_r = 1.44,\ q_x = 3.60,\ i^0_{L_{\rm inv}} = 3.19,\ i^0_{L_{\rm rec}} = -2.42$$

that using (3) leads to

$$L_{\rm inv} = 0\,{\rm H},\ L_p = 8.7\,\mu{\rm H},\ L_{\rm rec} = 2.2\,\mu{\rm H},$$
$$C_{\rm inv} = 4.0\,{\rm nF},\ C_{\rm rec} = 3.7\,{\rm nF}$$

for $f_s = 1.4\,{\rm MHz}$. The second harmonic solution is

$$q_i = 3.27,\ q_r = 2.05,\ q_x = 1.45,\ i^0_{L_{\rm inv}} = 2.92,\ i^0_{L_{\rm rec}} = -1.62$$

that is denormalized as

$$L_{\rm inv} = 0\,{\rm H},\ L_p = 8.7\,\mu{\rm H},\ L_{\rm rec} = 2.2\,\mu{\rm H},$$
$$C_{\rm inv} = 4.1\,{\rm nF},\ C_{\rm rec} = 6.5\,{\rm nF}$$

for $f_s = 568\,{\rm kHz}$. As expected, since we are working with constant inductors values, the second harmonic solution requires a working frequency lower by a $2.46\times$ factor.

The results of the SPICE simulation of both implementations are depicted in Fig. 4, showing for both solutions waveforms featuring optimal class-E condition. Interestingly, it is possible to verify that tuning the design on the second harmonic leads to a non-negligible advantage in terms of efficiency. For the first harmonic solution we have a 74.1% efficiency, that grows to 75.8% for the second harmonic one. The main source of losses is the diode (about $185\,{\rm mW}$ in both cases), while the losses on the resistive elements are larger in the first harmonic solution ($67\,{\rm mW}$ vs. $60\,{\rm mW}$ for the transformer, and $62\,{\rm mW}$ vs. $57\,{\rm mW}$ for the $L_{\rm rec}$) as expected from the theoretical analysis.

V. Conclusion

In this paper we have shown that the problem of designing a resonant converter according to optimal class-E conditions (i.e., ZVS and ZVDS), due to the non-linearity of the problem, may have multiple solutions. In particular, we are able to find two solutions, one tuned on the first harmonic of the clock, and the other one on the second harmonic. Both solutions has been investigated and compared. The second harmonic one shows some advantages such as the possibility of using either smaller magnetic elements or a lower working frequency, and a non-negligible increase in efficiency.

REFERENCES

[1] N. Sokal and A. Sokal, "Class E-A new class of high-efficiency tuned single-ended switching power amplifiers," *IEEE J. Solid-State Circuits*, vol. 10, no. 3, pp. 168–176, Jun. 1975.

[2] D. Perreault, J. Hu, J. Rivas, Y. Han, O. Leitermann, R. Pilawa-Podgurski, A. Sagneri, and C. Sullivan, "Opportunities and Challenges in Very High Frequency Power Conversion," in *24th Annu. IEEE Applied Power Electronics Conf. and Expo. (APEC2009)*, Feb 2009, pp. 1–14.

[3] J. M. Burkhart, R. Korsunsky, and D. J. Perreault, "Design Methodology for a Very High Frequency Resonant Boost Converter," *IEEE Trans. Power Electron.*, vol. 28, no. 4, pp. 1929–1937, Apr. 2013.

[4] M. Hayati, A. Lotfi, M. K. Kazimierczuk, and H. Sekiya, "Generalized design considerations and analysis of class-e amplifier for sinusoidal and square input voltage waveforms," *IEEE Transactions on Industrial Electronics*, vol. 62, no. 1, pp. 211–220, Jan 2015.

[5] R. Gutmann, "Application of RF Circuit Design Principles to Distributed Power Converters," *IEEE Trans. Ind. Electron. and Control Instr.*, vol. IECI-27, no. 3, pp. 156–164, Aug. 1980.

[6] J. W. Yang and H. L. Do, "Soft-switching dual-flyback dc-dc converter with improved efficiency and reduced output ripple current," *IEEE Transactions on Industrial Electronics*, vol. 64, no. 5, pp. 3587–3594, May 2017.

[7] G. Chen, Y. Deng, Y. Tao, X. He, Y. Wang, and Y. Hu, "Topology derivation and generalized analysis of zero-voltage-switching synchronous dc-dc converters with coupled inductors," *IEEE Transactions on Industrial Electronics*, vol. 63, no. 8, pp. 4805–4815, Aug 2016.

[8] N. Bertoni, G. Frattini, R. Massolini, F. Pareschi, R. Rovatti, and G. Setti, "An Analytical Approach for the Design of Class-E Resonant DC-DC Converters," *IEEE Trans. Power Electron.*, vol. 31, no. 11, pp. 7701–7713, Nov. 2016.

[9] F. Pareschi, R. Rovatti, and G. Setti, "Emi reduction via spread spectrum in dc/dc converters: State of the art, optimization, and tradeoffs," *IEEE Access*, vol. 3, pp. 2857–2874, 2015.

[10] F. Pareschi, G. Setti, and R. Rovatti, "A 3-ghz serial ata spread-spectrum clock generator employing a chaotic pam modulation," *IEEE Transactions on Circuits and Systems I: Regular Papers*, vol. 57, no. 10, pp. 2577–2587, Oct 2010.

[11] F. Pareschi, G. Setti, R. Rovatti, and G. Frattini, "Practical optimization of emi reduction in spread spectrum clock generators with application to switching dc/dc converters," *IEEE Transactions on Power Electronics*, vol. 29, no. 9, pp. 4646–4657, Sep. 2014.

[12] H. Sekiya, T. Ezawa, and Y. Tanji, "Design procedure for class e switching circuits allowing implicit circuit equations," *IEEE Transactions on Circuits and Systems I: Regular Papers*, vol. 55, no. 11, pp. 3688–3696, Dec 2008.

[13] S. Aldhaher, D. C. Yates, and P. D. Mitcheson, "Modeling and analysis of class ef and class e/f inverters with series-tuned resonant networks," *IEEE Transactions on Power Electronics*, vol. 31, no. 5, pp. 3415–3430, May 2016.

[14] J. Rivas, O. Leitermann, Y. Han, and D. Perreault, "A very high frequency dc-dc converter based on a class ϕ_2 resonant inverter," *IEEE Trans. Power Electron.*, vol. 26, no. 10, pp. 2980–2992, Oct 2011.

[15] Y. Cao, R. A. Groves, X. Huang, N. D. Zamdmer, J. . Plouchart, R. A. Wachnik, T.-J. King, and C. Hu, "Frequency-independent equivalent-circuit model for on-chip spiral inductors," *IEEE Journal of Solid-State Circuits*, vol. 38, no. 3, pp. 419–426, March 2003.